



Experimental screening of metal nitrides hydrolysis for green ammonia synthesis via solar thermochemical looping

Stéphane Abanades, Bertrand Rebiere, Martin Drobek, A. Julbe

► To cite this version:

Stéphane Abanades, Bertrand Rebiere, Martin Drobek, A. Julbe. Experimental screening of metal nitrides hydrolysis for green ammonia synthesis via solar thermochemical looping. *Chemical Engineering Science*, 2024, 283, pp.119406. 10.1016/j.ces.2023.119406 . hal-04251780

HAL Id: hal-04251780

<https://hal.science/hal-04251780v1>

Submitted on 20 Oct 2023

HAL is a multi-disciplinary open access archive for the deposit and dissemination of scientific research documents, whether they are published or not. The documents may come from teaching and research institutions in France or abroad, or from public or private research centers.

L'archive ouverte pluridisciplinaire **HAL**, est destinée au dépôt et à la diffusion de documents scientifiques de niveau recherche, publiés ou non, émanant des établissements d'enseignement et de recherche français ou étrangers, des laboratoires publics ou privés.

Experimental screening of metal nitrides hydrolysis for green ammonia synthesis via solar thermochemical looping

Stéphane Abanades^{1*}, Bertrand Rebiere², Martin Drobek², Anne Julbe²

¹ CNRS; Processes, Materials and Solar Energy laboratory (PROMES); 7 rue du Four Solaire; 66120 Odeillo Font-Romeu; France

² Institut Européen des Membranes (IEM); CNRS, ENSCM, Univ Montpellier; Place Eugène Bataillon; 34095 Montpellier; France

* Corresponding author: stephane.abanades@promes.cnrs.fr

Abstract

Ammonia is a fundamental chemical commodity for fertilizer and as a novel energy vector. Solar-driven ammonia synthesis is proposed as a sustainable alternative to the catalytic energy-intensive and CO₂-emitting Haber-Bosch process. The considered thermochemical process aims to produce ammonia from nitrogen and water ($\text{N}_2 + 3\text{H}_2\text{O} \rightarrow 2\text{NH}_3 + 1.5\text{O}_2$) via redox cycles using a solar heat source, thus bypassing the supply of H₂ or electricity. Metal oxide/nitride redox pairs can be employed for this cyclic process. The exothermal hydrolysis reaction of nitrides produces ammonia ($\text{M}_x\text{N}_y + 3\text{H}_2\text{O} \rightarrow 2\text{NH}_3 + \text{M}_x\text{O}_y$), and is followed by one or several regeneration steps ($\text{M}_x\text{O}_y + \text{N}_2 \rightarrow \text{M}_x\text{N}_y + 3/2\text{O}_2$) requiring a heat supply from concentrated solar energy. This study aims to experimentally identify the most suitable metal nitrides in the hydrolysis step for ammonia synthesis based on solar-driven chemical-looping. As a result, FeN, CrN, BN, and Si₃N₄ turned out to be irrelevant candidates for NH₃ production, as the hydrolysis yield was poor up to 1000°C. In contrast, AlN, Li₃N, Ca₃N₂, Mg₃N₂, TiN, and ZrN exhibited noteworthy reactivity depending on the temperature. The hydrolysis rate of AlN was significantly enhanced only above 1100°C, TiN showed an increasing NH₃ production rate with temperature (reaching 3.4 mmol/min/g at 1000°C), while an optimum at 750°C was unveiled for complete ZrN conversion (corresponding to the highest rate of 34.2 mmol/min/g). Hydrolysis of Li₃N, Ca₃N₂, and Mg₃N₂ was complete at lower temperatures (~200°C), with NH₃ yields of 5.9, 4.9, and 18.6 mmol/g, respectively. Solar-driven regeneration of metal nitrides at high temperature will be then necessary to demonstrate the complete feasibility of thermochemical cycles for green ammonia synthesis.

Keywords: ammonia synthesis, solar fuel, metal nitrides, chemical-looping, thermochemical cycles, hydrogen carrier.

1. Introduction

Ammonia is one of the most produced industrial chemical compounds with a current production of 168.1 million tons and annual growth of more than 2% to reach 197.2 million tons in 2026 (Mordor Intelligence LLP, 2021). Ammonia is a fundamental component of ammonium nitrate fertilizer. Hence, the main application sector is that of fertilizers for agriculture, while new applications as an energy carrier or as an effective means of hydrogen storage (Aziz et al., 2020) show a growing interest in proposing alternatives to fossil fuels. An increasing demand in ammonia is thus foreseen in the future. Ammonia as a clean fuel (and hydrogen carrier/vector) is promising since it can be stored more easily than hydrogen in the liquid form (NH₃ boiling point = -33.4 °C at 1 atm versus -253 °C for H₂) and it offers a higher volumetric energy density (12.7 MJ/L) than liquid hydrogen (8.5 MJ/L). Furthermore, vast ammonia infrastructure already exists due to its extensive use for fertilizers.

The search for carbon-free alternatives and less energy-intensive solutions for NH₃ production represents a major challenge for the years to come. Indeed, ammonia is currently produced by the Haber-Bosch process ($\text{N}_{2(g)} + 3\text{H}_{2(g)} \rightleftharpoons 2\text{NH}_{3(g)}$, $\Delta H^\circ = -91.9 \text{ kJ mol}^{-1}$) developed more than a century ago, which is highly energy-intensive and generates greenhouse gas (GHG) emissions (2.2 tons CO₂ / ton NH₃ (Rafiqul et al., 2005)). The ammonia production represents about 2% of the world consumption of fossil energy and generates over 420 million tons of

CO₂ per year, thus representing 1.2% of global anthropic CO₂ emissions (Liu et al., 2020). The Haber-Bosch process consists in reacting hydrogen (H₂) with nitrogen (N₂) using catalysts at high temperatures and pressures (400/650°C – 200/400 bars) and relies on fossil fuels. Indeed, the hydrogen required for the synthesis of ammonia is currently produced by steam reforming of natural gas, while N₂ is obtained by cryogenic separation of air. Both of these processes require a large input of energy, causing significant concomitant GHG emissions. Specific studies have been proposed to improve the efficiency of NH₃ synthesis unit by associating a tri-reforming reactor with a membrane unit (Damanabi et al., 2019). However, the use of ammonia as an energy carrier cannot be considered as a decarbonized source when using hydrogen of fossil origin. It is thus necessary to develop alternatives to the Haber-Bosch process. In order to make ammonia a sustainable energy carrier in the future, the decarbonation of its production and the use of a renewable energy source are necessary. The decarbonation of ammonia production can be achieved by using green hydrogen (produced by electrolysis) or by directly producing ammonia via new electrochemical or thermochemical processes. However, with the increasing deployment of hydrogen as an energy carrier in the transport sector or for industrial applications (e.g., for direct reduced iron and steel metallurgy (Bhaskar et al., 2020; Patisson and Mirgaux, 2020)), it becomes necessary to develop alternatives for ammonia production in order to avoid consuming the green hydrogen feedstocks that will be produced. The direct use of H₂ in the process should therefore be avoided, while preferring production from nitrogen and water.

To avoid using the Haber-Bosch process, the synthesis of ammonia from renewable energies must be developed on an industrial scale (Wang et al., 2018). Accordingly, the primary energy source can be used either in the form of electricity or in the form of heat. The solar-driven production of ammonia by directly using the heat generated by solar concentrating systems with a higher energy conversion efficiency than electrolysis (because it is not limited by the efficiency of the intermediate electricity production) appears to be an ideal solution (Abanades, 2023). This method is advantageous because it can potentially produce ammonia from N₂ and H₂O without electricity input or hydrogen consumption. The overall reaction is however highly endothermic ($\text{N}_2 + 3\text{H}_2\text{O} \rightarrow 2\text{NH}_3 + \frac{3}{2}\text{O}_2$, $\Delta H^\circ = 633.6 \text{ kJ/mol}$), it cannot occur spontaneously due to the high stability of nitrogen and requires a significant energy input (either heat or electricity). Therefore, the use of concentrated solar energy for providing the reaction enthalpy represents a major interest. This reaction corresponds to the reverse of NH₃ combustion, achievable thanks to contribution of solar energy.

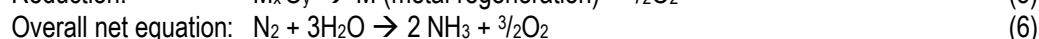
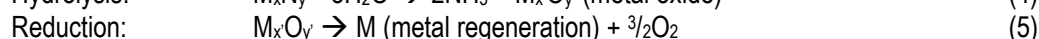
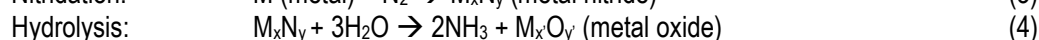
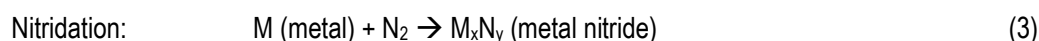
Various alternative methods of ammonia production under mild conditions have been proposed, especially for solar energy integration in low-pressure green ammonia production technologies (Klaas et al., 2021). Possible processes include solid state synthesis, molten salt synthesis, thermochemical looping and photocatalytic routes. Electrochemical processes based on green electricity produced by renewable energies have been studied to synthesize ammonia, among which one can cite solid-state ammonia synthesis (SSAS) (Kishira et al., 2017; Kyriakou et al., 2017; Marnellos et al., 2000; Marnellos and Stoukides, 1998; Qing et al., 2016) or synthesis by means of molten salts (Murakami et al., 2005a, 2005b, 2003). Such electrochemical processes require electrodes and an electrolyte (solid or molten salts) and have the advantage of not requiring high pressures. However, in some electrochemical processes, the synthesis still makes use of N₂ and H₂, it is thus necessary to privilege the processes rather based on the use of N₂ and water. Among the main drawbacks of such processes, it can be noticed that the electrodes generally include noble metals (Pd, Pt, Ru) (Ceballos et al., 2021), the NH₃ production rates are low, and the overall efficiency of the process remains limited by the conversion of the primary energy source into electricity. Other routes have considered the chemical looping of metal nitrides consisting of a reduction of N₂ with a looped metal nitride ($\text{M}_a\text{N}_{b-\delta} + \delta/2 \text{ N}_2 \rightarrow \text{M}_a\text{N}_b$), followed by separate hydrogenation of the lattice nitrogen in ammonia ($\text{M}_a\text{N}_b + 3\delta/2 \text{ H}_2 \rightarrow \text{M}_a\text{N}_{b-\delta} + \delta \text{ NH}_3$) (Daisley and Hargreaves, 2023; Goto et al., 2021; Hunter et al., 2010; Laassiri et al., 2018; Michalsky et al., 2015a; Yang et al., 2022). However, such a process still relies on the use of H₂ as feedstock, since the net reaction remains unchanged ($\text{N}_2 + 3\text{H}_2 \rightarrow 2\text{NH}_3$), and the exothermicity of this global reaction makes the use of solar energy less attractive.

As an alternative to the Haber-Bosch process and the electrochemical synthesis of ammonia, this study aims to develop thermochemical processes for the production of ammonia from N₂ and H₂O, using concentrated solar energy as a high-temperature heat source. Previous works have already been devoted to the development of solar-driven thermochemical redox cycles for water splitting to produce hydrogen (Abanades, 2022; Haeussler et al., 2019; Le Gal and Abanades, 2011; Xiao et al., 2012). Reduction of metal oxides using high-temperature solar heat has also been proved to be feasible (Chambon et al., 2010a, 2010b; Chuayboon and Abanades, 2019). Similarly, metal oxide/nitride redox cycles can be proposed. Chemical-looping ammonia production pathways have been

reviewed (Lai et al., 2022). The ammonia synthesis reaction from water and nitrogen can be decomposed into several steps, with high-temperature heat supplied by concentrated solar radiation as the only energy input. Such cycles for solar thermochemical ammonia production can be operated in two or three steps, using different reactive intermediate materials participating in the reactions. This makes possible the ammonia synthesis under milder conditions (atmospheric pressure and temperatures compatible with concentrated solar energy). For instance, two-step cycles involve a reaction of metal nitride with water vapour to produce ammonia and the metal oxide (Eq. 1), followed by an endothermic step (Eq. 2) corresponding to the regeneration of metal nitride from the nitridation reaction of the oxide with N₂ (and with the potential support of a reducing agent such as C, CH₄, biomass).



A three-step cycle based on the metal oxide/nitride redox pair can also be considered with the same overall net reaction (Klaas et al., 2021) (note that equations are not balanced as they depend on the redox pair involved):



The main advantages of such cycles include: (i) the absence of a fossil energy source allowing the decarbonation of ammonia production, (ii) the use of hydrogen as a reactant is not required, (iii) the reaction carried out at atmospheric pressure, (iv) the absence of expensive catalysts and material consumption as the reactive materials are cycled, (iv) the direct use of solar energy as a process heat source without intermediate production of electricity, thereby enhancing overall energy conversion efficiencies. Recent theoretical studies have identified possible oxide/nitride redox couples (Bartel et al., 2019), but to date very few experimental studies have demonstrated the feasibility of solar ammonia production by thermochemical cycles. Nitrides of chromium, aluminum, lithium, molybdenum and manganese were previously proposed and studied experimentally (Gálvez et al., 2008; Jain et al., 2017; Michalsky et al., 2015b; Michalsky and Pfromm, 2011). However, there is no available comprehensive experimental study comparing the ability of various nitrides to produce ammonia. In addition, high-throughput equilibrium analysis and computational screening were also performed for rapid identification of candidate materials (Bartel et al., 2019; Michalsky and Steinfeld, 2017). Regarding the synthesis of nitrides (regeneration step), the solar carbothermal reduction of metal oxides (Al₂O₃, SiO₂, TiO₂, and ZrO₂) in N₂ to produce nitrides was demonstrated (Murray et al., 1995), which confirmed the feasibility of nitrides synthesis from their oxides at high temperatures with the addition of a reducing agent. The economics and scale-up ability of the technology have been assessed (Gálvez et al., 2007b; Michalsky et al., 2012).

Solar ammonia production via thermochemical cycles based on metal nitrides is a suitable means for the decarbonation of the industrial process, reducing both its environmental impact and its energy/economic costs. Several innovative aspects of this approach can be mentioned. The solar process considered for ammonia production avoids the direct use of hydrogen as a feedstock, while being a green process without electricity supply. The cycles are solely based on metal nitrides as intermediate compounds and on solar heat for NH₃ production from N₂ and H₂O as the only feedstocks. The development of active metal nitride materials for the hydrolysis step to synthesize NH₃ with high yields and the high-temperature solar-driven regeneration for the nitridation step are the main challenges for process performance enhancement, paving the way to industrial applications.

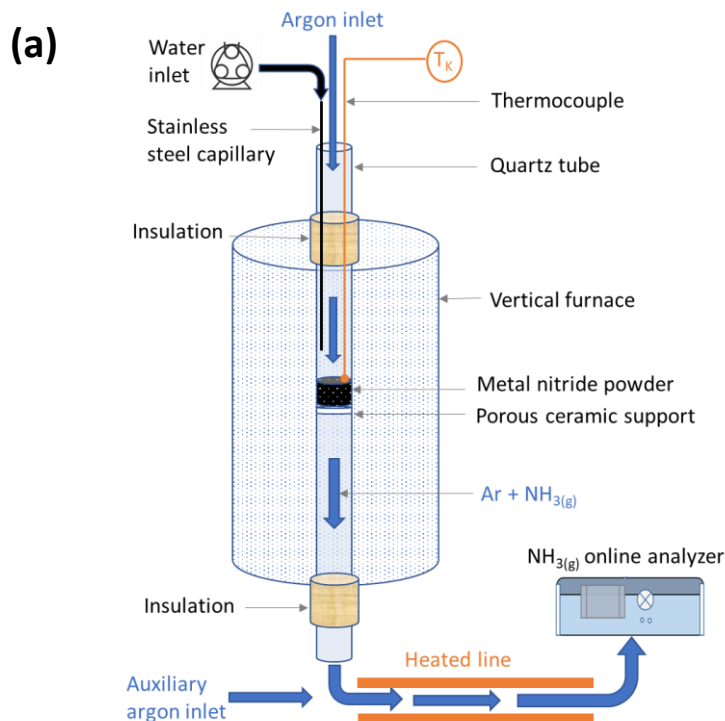
In particular, the reactivity of nitrides during hydrolysis must first be demonstrated experimentally to identify suitable candidates for solar ammonia synthesis. Experimental screening of metal nitrides hydrolysis has never been done before. There is no study comparing the reactivity of different nitrides in the literature. In addition, their ability to produce ammonia during hydrolysis must be quantified and suitable operating conditions must be identified for each candidate material. In this study, a series of metal nitrides was thus selected for an experimental screening of their reactivity towards the production of NH₃. The aim was to identify the most suitable metal nitrides in the hydrolysis step to synthesize NH₃ with high yields and production rates. The reaction conversion, hydrolysis rate, and ammonia production capacity were evaluated by investigating the direct reaction of nitride powders with steam in a packed-bed reactor, and the influence of temperature was probed. Ammonia production was directly measured and quantified via continuous evolved gas analysis. Active metal nitride candidates with their corresponding performance for ammonia synthesis were identified.

2. Experimental set-up and methods

2.1 Experimental bench

An experimental bench dedicated to the study of the hydrolysis step of metal nitrides with continuous evolved gas analysis has been specifically developed to perform nitrides screening and compare NH_3 production rates. The experimental set-up (Figure 1) is composed of a vertical tubular furnace to study the production of NH_3 at different temperatures. A tubular quartz reactor is placed inside the furnace. The metal nitride powder is loaded as a packed-bed ($\sim 0.1\text{--}0.5\text{ g}$) inside the vertical tubular furnace in the center of the quartz tube (16 mm inside diameter, middle of the tube 175 mm from the ends) and supported by a porous ceramic (zirconia felt).

The reactor is connected to a gas inlet to inject the carrier gas (Ar, 99.999% purity) with a flow-rate controlled by a mass-flow controller (MFC, Brooks, range 0-1 NL/min). A stainless-steel capillary is placed inside the quartz tube to inject water vapor using a calibrated peristaltic pump (for liquid water flow-rate control). The water is then vaporized as it flows through the capillary and exits as steam which is transported by the Ar carrier gas through the powder bed. At the quartz tube outlet, a heated line ($T > 120^\circ\text{C}$) is used to sample the exhaust gases towards an NH_3 analyzer, avoiding any condensation of steam in which the soluble NH_3 could be trapped. On this outlet, an auxiliary Ar input (MFC, Brooks, range 0-5 NL/min) is connected for the dilution of the NH_3 concentration in order to maintain it within the detection range of the analyzer. The maximum NH_3 concentration reached also depends on the initial mass of loaded nitride in the reactor, which must be thus controlled to avoid peak saturation. The exiting gas is analyzed using a dedicated UV-vis spectrophotometer (OMA-406, Applied Analytics, measurement cell heated to 150°C , range: 0-10000 ppm, calibrated with 5000 ppm NH_3 calibration gas) to continuously measure the ammonia concentration during hydrolysis and monitor the progress of the reaction (one measurement performed every 5 s). The reaction temperature is measured by a K-type thermocouple reaching inside the powder bed. Both the sample bed temperature and the NH_3 concentration are recorded continuously by data acquisition with a time step of 1 s.



(b)

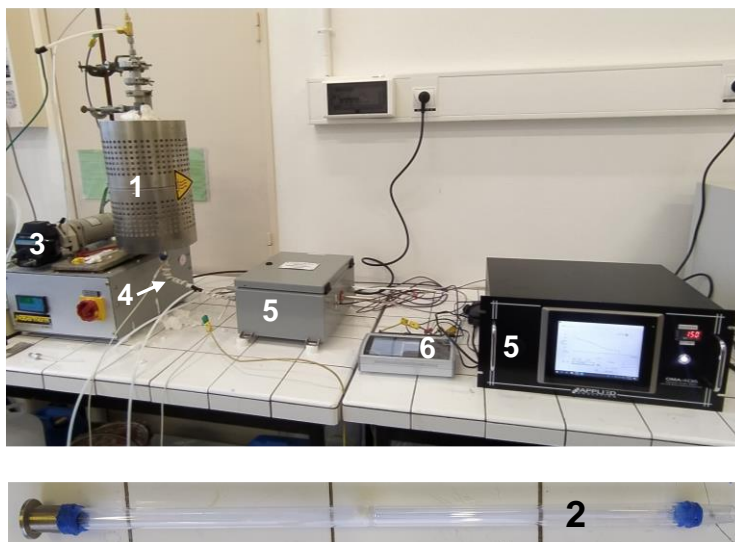
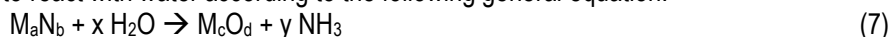


Figure 1. Experimental hydrolysis reactor and set-up: (a) Schematic of the packed-bed of commercial nitride powder in a vertical tubular furnace with continuous NH_3 analysis in the exit gas, (b) Photograph of the set-up (1. Tubular furnace; 2. Quartz tube reactor; 3. Peristaltic pump; 4. Heated line; 5. NH_3 analyzer; 6. Acquisition system).

2.2 Materials and methods

A series of ten commercial metal nitrides (Sigma Aldrich) was selected to investigate the hydrolysis reaction: AlN (purity $\geq 98\%$, metals basis), Li_3N (99.4%), Ca_3N_2 (99%), Mg_3N_2 (99.6%), TiN ($\geq 99.7\%$), CrN ($\text{Cr}_2\text{N} + \text{CrN}$, $\geq 99.5\%$), Fe_xN ($x=2-4$, $\geq 99.7\%$), BN ($\geq 99.7\%$), Si_3N_4 (99.9%), and ZrN (99.5%).

These materials are expected to react with water according to the following general equation:



Each material was thus tested during the hydrolysis reaction to compare the NH_3 production yields and the reaction rates at different temperatures.

The nitridation step was not studied in this work, but the carbothermal reduction of oxides in the presence of N_2 appears to be a favorable route for the regeneration of nitrides. For instance, the combined carbothermal reduction and nitridation of Al_2O_3 , TiO_2 , SiO_2 and ZrO_2 oxides are thermodynamically possible upon increasing temperature based on their Gibbs free enthalpy variation (Murray et al., 1995).

The experimental conditions are summarized in Table S1 (Supplementary Information). The Ar carrier gas flow-rate was set at 0.2 NL/min and the water vapor flow-rate was 0.224 NL/min. The resulting steam molar content in the reactor was therefore 52.8%. At the reactor outlet, the gas was diluted with Ar (typically 1.25 NL/min) before being injected into the analyzer to avoid saturation of the analysis cell and to remain within the suitable measurement range of the gas analysis system (0-10000 ppm). The nitride mass loaded in the reactor was thus maintained low enough to avoid excessively high ammonia concentrations in the outlet gas and to prevent signal saturation, thus warranting reliable online analysis. The amount of NH_3 evolved from the hydrolysis reactions was quantified, as detailed in the following. The NH_3 mole fraction (y_{NH_3}) was measured as a function of time. From these data, the production rate and the total amount of NH_3 can be calculated as follows:

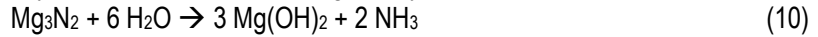
$$Q_{\text{NH}_3} = \frac{y_{\text{NH}_3} \cdot Q_{\text{total}}}{m_{\text{nitride}}} \quad (8)$$

with Q_{NH_3} the NH_3 production rate per unit mass of nitride ($\text{mol} \cdot \text{min}^{-1} \cdot \text{g}^{-1}$), y_{NH_3} the NH_3 mole fraction at the reactor outlet, Q_{total} the total outlet gas molar flow-rate after dilution (mol/min), and m_{nitride} the nitride mass loaded into the reactor (g).

Q_{total} depends on the studied nitride and the corresponding global reaction equation of the hydrolysis. Indeed, part of the injected steam is consumed during the reaction producing NH_3 . The outlet gas flow-rate corresponds to the sum of the outlet flow-rates of argon (Q_{Ar}), unreacted steam ($Q_{\text{H}_2\text{O,outlet}}$) and NH_3 , and is therefore expressed by:

$$Q_{\text{total}} = Q_{\text{Ar}} + Q_{\text{H}_2\text{O},\text{outlet}} + m_{\text{nitride}} \cdot Q_{\text{NH}_3} \quad (9)$$

For example, in the case of Mg_3N_2 hydrolysis, the overall equation is given by:



The flow-rate of unreacted steam can then be calculated as follows:

$$Q_{\text{H}_2\text{O},\text{outlet}} = Q_{\text{H}_2\text{O},\text{inlet}} - 3 \cdot Q_{\text{NH}_3} \quad (11)$$

By combining Eqs. (8), (9), and (11), Q_{NH_3} can be expressed as:

$$Q_{\text{NH}_3} = \frac{y_{\text{NH}_3} \cdot (Q_{\text{Ar}} + Q_{\text{H}_2\text{O},\text{inlet}})}{(1 + 2y_{\text{NH}_3}) \cdot m_{\text{nitride}}} \quad (12)$$

The total amount of NH_3 produced (mol/g) is calculated by integrating the NH_3 molar flow-rate over the hydrolysis step duration.

$$n_{\text{NH}_3} = \int_0^t Q_{\text{NH}_3} \cdot dt \quad (13)$$

The performance metrics including global amounts of generated ammonia and production rates were expressed per unit mass of metal nitride (Eq. 8 and Eq. 13) for comparison purpose on the same basis.

The ammonia yield can then be obtained from:

$$X_{\text{NH}_3} = \frac{n_{\text{NH}_3}}{n_{\text{NH}_3,\text{max}}} \quad (14)$$

where $n_{\text{NH}_3,\text{max}}$ is the theoretical maximum amount of NH_3 calculated from the overall reaction equation.

In addition, the structure and microstructure of fresh and hydrolyzed materials were characterized by different techniques to verify the powders conversion and to confirm that the reactions occur as expected.

Crystalline structure and phase identification were studied by X-ray diffraction (XRD) using a Panalytical X'PERT PRO diffractometer with the Cu K α radiation ($\alpha_{\text{Cu}} = 0.15406 \text{ nm}$, angular range = $20\text{--}80^\circ$, 2θ , tube current 20 mA, potential 40 kV).

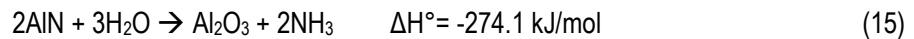
The morphology of the materials was observed with a Field Emission Scanning Electron Microscope (FESEM - Hitachi S4800) used to examine /compare the microstructure of the powders. An elemental chemical analysis cartography was carried out by EDX analysis (Energy Dispersive X-ray Spectroscopy, using a Zeiss Sigma 300 with an accelerating voltage of 15 keV) to estimate the chemical composition and observe elements distribution (surface mapping) in the materials.

In total, 44 hydrolysis runs were carried out with the experimental set-up in order to characterize the series of 10 metal nitrides considered (Table S1).

3. Results and discussion

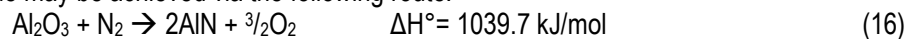
3.1 Aluminum nitride (AlN)

The hydrolysis of AlN can be written:



The theoretical production corresponds to one mole of NH_3 per mole AlN, i.e., 24.4 mmol/g or 546.5 mL/g (based on the H_2 equivalence, this corresponds to 36.6 mmol H_2 /g).

The regeneration of the nitride may be achieved via the following route:



This highly endothermic reaction is not thermodynamically favorable and the addition of a carbonaceous reducing agent (carbon or methane (Gálvez et al., 2008, 2007b, 2007a)) is necessary according to:





The solar-driven carbothermal reduction of Al_2O_3 in N_2 atmosphere has also been studied (Murray et al., 1995).

Figure 2 shows the equilibrium composition of the $2\text{AlN} + 3\text{H}_2\text{O}$ system (Eq. 15) as a function of temperature at 1 bar. The hydrolysis reaction producing ammonia is thermodynamically favorable at low temperature (below $\sim 200^\circ\text{C}$), whereas NH_3 is not stable above 300°C as it decomposes into H_2 and N_2 although a metastable state may exist without the presence of catalysts. It should be noted that similar thermodynamic equilibrium distributions are obtained regardless of the metal nitride considered, with NH_3 being stable only below 300°C .

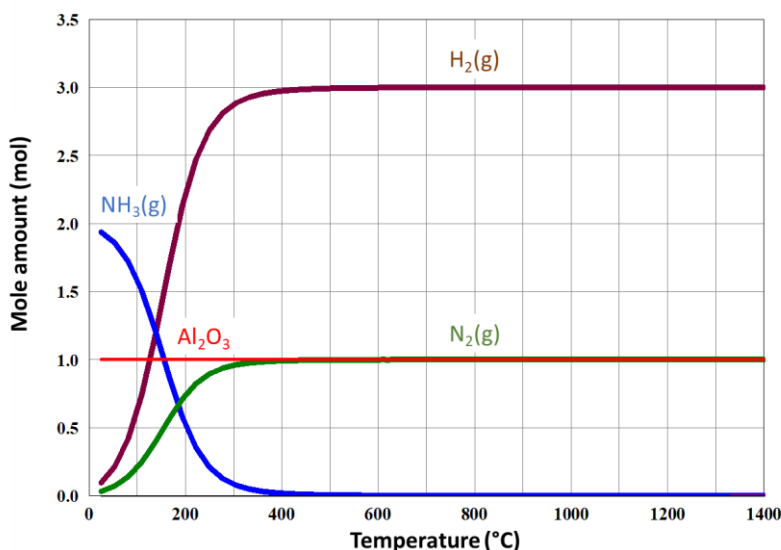


Figure 2. Thermodynamic equilibrium composition of the $2\text{AlN} + 3\text{H}_2\text{O}$ system as a function of the temperature at 1 bar.

A series of ten AlN hydrolysis runs was carried out at temperatures ranging from 200°C to 1200°C . Repeatability of the results was confirmed through different tests with similar conditions. The initial AlN mass did not significantly affect the mass-specific amount of ammonia produced (e.g., 1 mmol/g in run #13 vs. 1.1 mmol/g in run #14 at 1000°C). Increasing the temperature was found to significantly improve NH_3 production. Indeed, the NH_3 production rate was low below 1000°C , but it increased drastically above this temperature. This suggests that the reaction is hindered by kinetic limitations since the increase in temperature favors the reaction kinetics, although the reaction is not thermodynamically favorable at high temperatures. Actually, the slow kinetics at low temperatures does not allow thermodynamic equilibrium to be reached in a reasonable reaction time. Figure S1 represents the evolution of the NH_3 production rate at 550°C and 960°C . NH_3 was detected right from the steam was injected, with total production yields (n_{NH_3}) of 0.66 and 0.77 mmol/g, respectively. The NH_3 concentration reached a peak promptly then gradually decreased until reaching negligible values. During AlN sample heating, a weak NH_3 production was measured around 200°C even in the absence of H_2O (Fig. S1b), which suggests a reaction of AlN with residual moisture.

Figure 3a shows the evolution of the NH_3 production rates at 1100°C (hydrolysis of 155 mg AlN) and 1200°C (hydrolysis of 156 mg AlN) as a function of time, which confirms the improved kinetics when increasing the temperature. During hydrolysis at 1200°C , the peak production rate of NH_3 reached $1.6 \cdot 10^{-4}$ mol/min/g versus $5 \cdot 10^{-5}$ mol/min/g at 1100°C . The total reaction duration decreased from about 40 min at 1100°C to 20 min at 1200°C . Therefore, heating the reactants favored the NH_3 production rate although the reaction was thermodynamically less favorable. The cumulative production of NH_3 reached about 1.1 mmol/g (which corresponds to an NH_3 yield X_{NH_3} of 4.5%). This total NH_3 yield remained almost unchanged whatever the temperature (Fig. 3b). The high temperature necessary to reach a significant hydrolysis rate (above 1000°C) can however represent an obstacle to the implementation of the $\text{Al}_2\text{O}_3/\text{AlN}$ redox system, given that the NH_3 yield is not improved above this temperature.

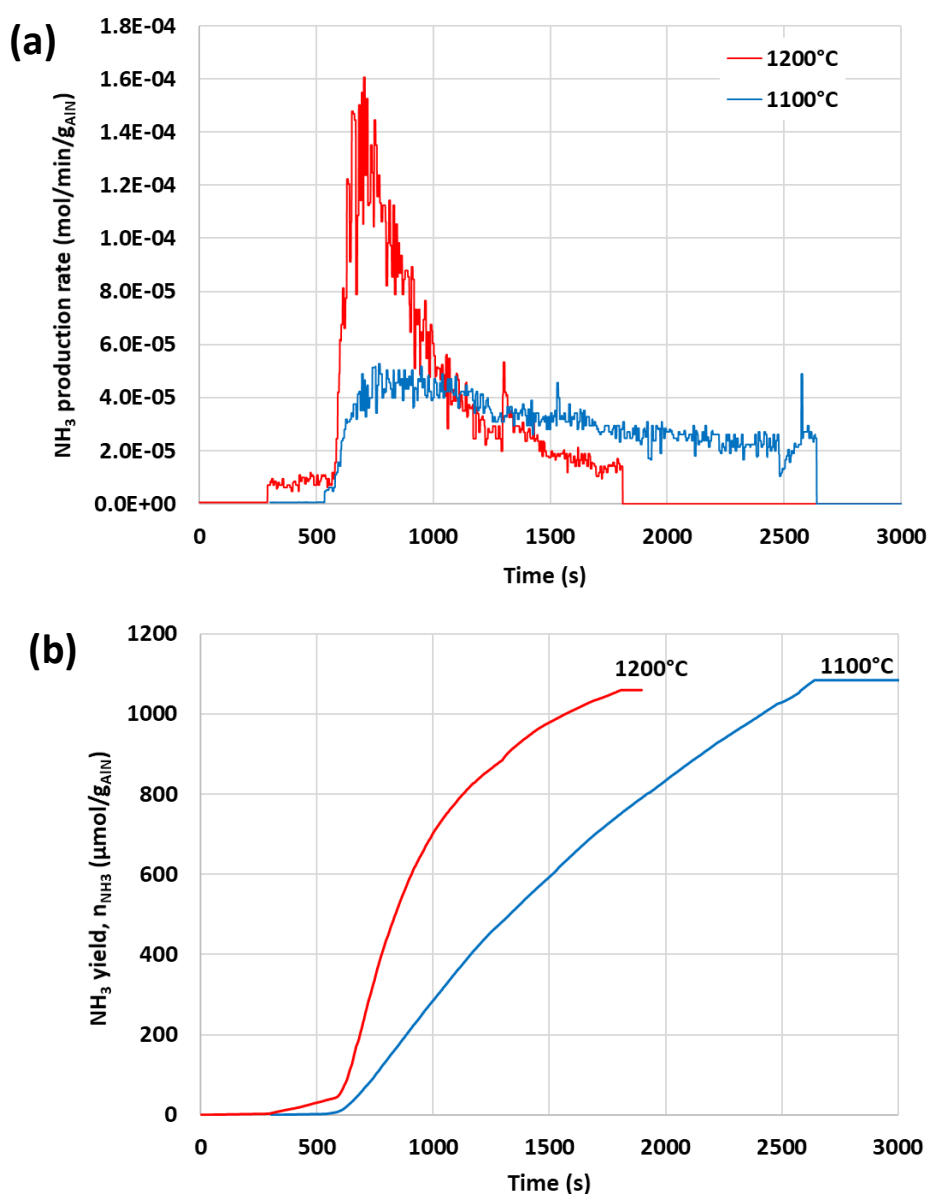


Figure 3. NH_3 production during AlN hydrolysis at 1100°C and 1200°C : (a) evolution of NH_3 production rate as a function of time, (b) cumulative NH_3 production as a function of time.

Characterization of the products was carried out to identify the main phases after the hydrolysis reaction and to confirm the oxidation of the nitrides during ammonia synthesis upon exposure to steam. XRD analysis of materials before and after two hydrolysis tests at 1000°C (Fig. 4) showed that the reaction was not complete because AlN was still present in majority after reaction in both tests. In contrast, the products analysis after AlN hydrolysis at 1100°C and 1200°C (Fig. S2) showed that Al_2O_3 was the main species with residual traces of AlN (in lower amount at 1200°C than at 1100°C), which confirmed the efficient conversion of AlN to Al_2O_3 . Some traces of ZrO_2 (tetragonal) were also identified due the zirconia felt used as support for the packed-bed of nitride powder during hydrolysis tests (this support could not be completely eliminated during the recovery of the packed-bed powder after reaction).

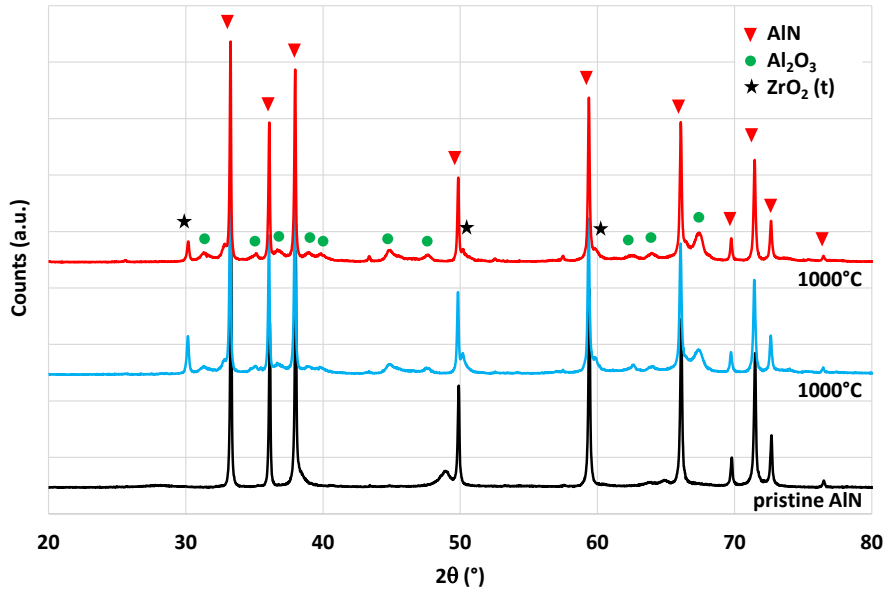
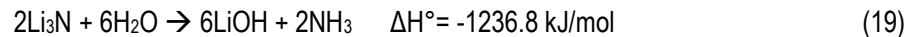


Figure 4. XRD patterns of AlN powders before and after hydrolysis at 1000°C.

A semi-quantitative EDX analysis was carried out for the powders collected after hydrolysis at 1100°C and 1200°C to confirm the complete conversion of the nitride during the reaction. Tables S2-3 report the atomic composition of the powders on different analysis zones (Figs. S3-4). For both temperatures, the Al/O ratio was close to the atomic composition of Al₂O₃ with Al/O = 0.57 at 1100°C and Al/O = 0.69 at 1200°C. The absence of nitrogen (below the detection limit) also denotes that AlN hydrolysis was complete at these temperatures and AlN was efficiently converted to Al₂O₃ after reaction. It should be noted that nitrogen is a light element that is difficult to detect and that it may be present in an amount lower than the detection limit of the analysis method. Figures S5 and S6 show SEM micrographs and X-ray elemental mapping of powders after hydrolysis at 1100°C and 1200°C. The distribution of Al and O is homogeneous, which means that these elements are evenly distributed over the sample surface. Although complete AlN conversion was observed above 1000°C, the NH₃ production yield was low compared to the maximum achievable value from Eq. (15), which is explained by the thermal instability of NH₃. Indeed, ammonia is not stable at high temperatures according to thermodynamics (Figure 2) and can decompose into N₂ and H₂. The NH₃ yield was therefore likely limited by the thermodynamically favorable dissociation of NH₃. These results are consistent with previous kinetic studies performed by thermogravimetric analysis (Gálvez et al., 2007a), in which a reaction conversion close to 95% was reported at 1100°C and 1200°C, and 68% at 950°C using a mixture 80% H₂O-Ar. However, the reaction rate was drastically reduced under 10% H₂O-Ar with a reaction extent of 40% at 1200°C after 20 min (complete reaction after ~100 min) and 20% at 1100°C after 30 min. This study also reported a maximum NH₃ yield of 88% obtained at 1000°C for a reaction extent of 93%, which decreased at higher temperatures. Importantly in this study, ammonia was not directly detected and measured by gas analysis, but indirectly quantified by mass balance.

3.2 Lithium nitride (Li₃N)

The synthesis of ammonia from lithium nitride was considered by Jain et al. (Jain et al., 2017), considering both the nitride hydrolysis reaction (Eq. 19) and the nitride regeneration.



The theoretical amount of NH₃ produced corresponds to one mole NH₃ per mole Li₃N, thus 28.7 mmol/g (642.9 mL/g) and 43.1 mmol_{H₂}/g relative to the H₂ equivalence. Lithium is a light element, which results in a high mass-specific NH₃ production potential, relative to the mass of material.

Figure 5a shows the evolution of the NH₃ production rate during Li₃N hydrolysis (107 mg) at 200°C. The reaction rate was fast and several successive peaks in NH₃ production were observed due to unstable steam injection caused by discontinuous droplet feeding. The hydrolysis reaction was completed in less than 2 min. The maximum NH₃ production rate reached 1.28.10⁻² mol/min/g and the total NH₃ yield reached 5.9 mmol/g (Figure 5b),

corresponding to a hydrolysis yield of 20.3%. A prompt and substantial increase in temperature (+80°C) was also observed during the reaction, which can be attributed to the heat generated by the strongly exothermic reaction. As a result, the product was sintered but could be recovered for solid phase characterization. According to XRD (Fig. S7), the Li_3N powder was totally converted after hydrolysis with the presence of LiOH phase. These results are in agreement with previous work on the reaction of lithium nitride with water vapor at 100°C showing major formation of NH_3 detected by gas chromatography (Jain et al., 2017).

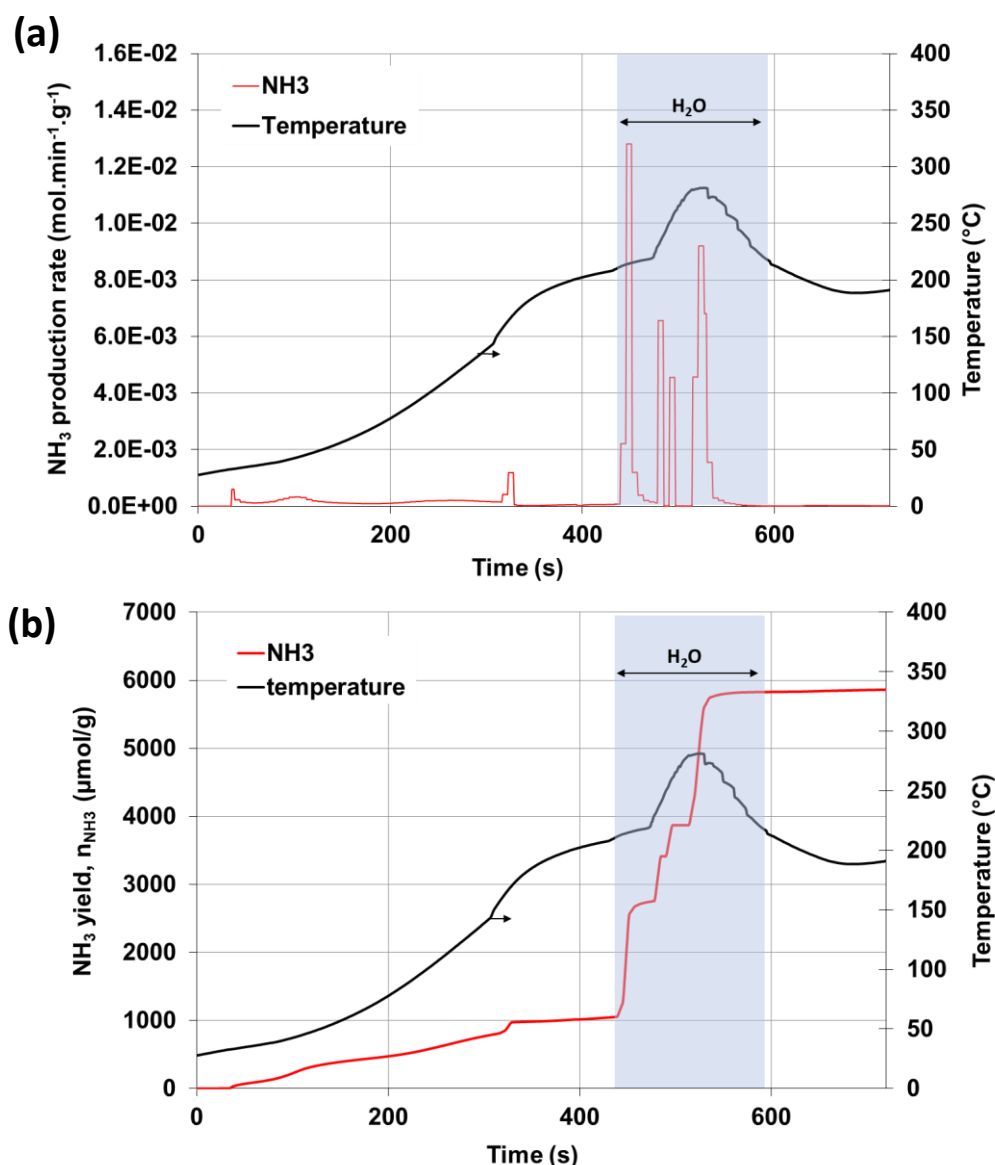


Figure 5. NH_3 production during Li_3N hydrolysis at 200°C: (a) evolution of NH_3 production rate as a function of time, (b) cumulative NH_3 production as a function of time.

3.3 Chromium ($\text{Cr}_2\text{N}/\text{CrN}$), boron (BN), iron (Fe_xN), and silicon (Si_3N_4) nitrides

Chromium, iron, boron, and silicon nitrides did not show a high reactivity during hydrolysis regardless of the temperature considered. Experimental results for the hydrolysis of these nitrides are given in the following without detailed characterization as they were not identified as suitable candidates for ammonia production.

Chromium nitride was previously considered for solar ammonia production (Michalsky and Pfromm, 2011). The reduction of Cr_2O_3 was carried out in N_2 with the help of a reducing agent such as CO or H_2 , resulting in the formation of a CrN and Cr_2N mixture. Then, a small amount of NH_3 was measured during hydrolysis in this previous work,

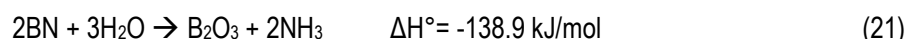
which was attributed to the slow corrosion kinetics of this nitride (also well known for its application as a protective coating).

The hydrolysis reaction can be written as follows:



The hydrolysis of commercial chromium nitride (520 mg) composed of a mixture of Cr_2N and CrN phases (Fig. S8, mean Cr/N atomic ratio of 1.7 measured by EDX) was investigated at temperatures of 570°C and 950°C. Figure S9a shows the NH_3 production profile as a function of time with steam injections at 570°C and 950°C. Whatever the temperature, the NH_3 production remained very low with peak production rates of 1.10^{-6} mol/min/g and $7.8.10^{-6}$ mol/min/g at 570°C and 950°C, respectively. The cumulated value of NH_3 production during CrN hydrolysis was also weak and did not exceed 10 $\mu\text{mol/g}$ (Figure S9b). These results are in agreement with previous studies (1.07×10^{-4} mol NH_3 /mol Cr/min reported by Michalsky and Pfromm, 2011) and the main reason for this low production was attributed to the preferential formation of N_2 by nitride decomposition instead of NH_3 formation.

Boron nitride was identified in a theoretical study as a potential candidate material for solar thermochemical NH_3 synthesis (Bartel et al., 2019). Equilibrium calculations identified the $\text{BN/B}_2\text{O}_3$ redox couple with the ability to produce 10 mmol NH_3 /g in one cycle.



In order to experimentally test the feasibility of ammonia synthesis, the hydrolysis of commercial boron nitride (198 mg) was carried out in this work at different temperatures (pure cubic BN phase was identified by XRD, Fig. S8). Figure S10a shows the NH_3 production profile at 370°C, 700°C, and 970°C. As a result, very weak production rates were observed at the lowest temperatures while a peak production rate of 1.10^{-5} mol/min/g was reached at 970°C. However, the cumulated production yield remained low with only 31 $\mu\text{mol}_{\text{NH}_3}$ /g (Figure S10b). After the reaction, the material was vaporized and could not be recovered. Therefore, contrary to theoretical predictions, boron nitride did not show suitable hydrolysis reactivity for ammonia synthesis at the different temperatures studied.

Iron nitride was also previously identified as a potential material for ammonia synthesis (Bartel et al., 2019) and was thus considered in this work. Commercial iron nitride is labeled with a Fe_xN composition (x in the range 2-4). A mean Fe/N atomic ratio of 3.2 was measured by EDX. A phase mixture of mainly Fe_4N with Fe_3N was identified by XRD (Fig. S8).

The NH_3 production profile from Fe_xN (400 mg) at 250°C, 550°C, and 1000°C is shown in Figure S11. At 250°C, no production was detected. At 550°C, a peak of NH_3 production was measured with a maximum value at $3.2.10^{-4}$ mol/min/g but no further NH_3 was significantly observed at 1000°C. The total cumulative production of NH_3 at 550°C was 230 $\mu\text{mol/g}$ (Figure S11b), which remains well below the theoretically predicted 10 mmol/g. In addition, part of the material was melted and sublimated after the test (rust-colored deposit on the walls of the quartz tube denoting the presence of Fe_2O_3).

XRD analysis of the material after hydrolysis was carried out (Figure S12), which revealed the presence of different iron oxide phases (FeO , Fe_2O_3 and Fe_3O_4), without any nitride phase being detected. This shows that NH_3 production is not correlated to the oxidation state of the material after hydrolysis. In other words, ammonia formation may not occur even if the material is fully oxidized after hydrolysis. The nitrogen released can indeed form species other than NH_3 (such as N_2) or NH_3 can be thermally decomposed before exiting the reactor.

Silicon nitride was studied to evaluate its reactivity toward NH_3 synthesis during hydrolysis.

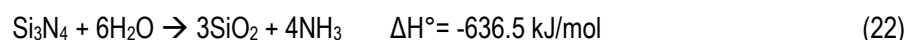


Figure S13a shows the NH_3 production profile during three consecutive hydrolysis tests of Si_3N_4 (322 mg) at 220°C, 520°C, and 980°C. Peaks of NH_3 production rate were observed at the three temperatures and reached 9.10^{-6} , $2.1.10^{-4}$ and $2.6.10^{-4}$ mol/min/g, respectively. The production rate was enhanced when the temperature increased. The cumulative amounts of NH_3 remained low for each temperature and were respectively 5, 65, and 183 $\mu\text{mol/g}$ (Figure S13b). According to XRD (Fig. S14), the Si_3N_4 phase was still the main one detected after hydrolysis, confirming the negligible nitride powder conversion.

3.4 Calcium nitride (Ca₃N₂)

The hydrolysis of calcium nitride has been thoroughly investigated given the good reactivity towards NH₃ synthesis.

The overall reaction equations are:



Based on Eq. (23), the theoretical maximum NH₃ production is 13.5.10⁻³ mol/g. Figure 6 shows the NH₃ production profile during Ca₃N₂ hydrolysis (100 mg) at 250°C. Calcium nitride is highly reactive during hydrolysis with a peak production rate of NH₃ reaching 5.2.10⁻³ mol/min/g and an overall reaction duration of about 10 min. Steam was injected at a reactor temperature of 250°C inducing a slight temperature increase (260°C) due to the exothermal reaction, but strong temperature variations between 170°C and 90°C were then observed, which can be explained by the energy consumed by the vaporization of water and falling droplets on the thermocouple. Figure 6b plots the cumulative production of NH₃ during Ca₃N₂ hydrolysis, reaching a value of 4.9.10⁻³ mol/g in less than 10 min (corresponding to 36.5% of the theoretical maximum production). The strong temperature drop during hydrolysis (up to ~100°C) may be responsible for the incomplete NH₃ yield. Additional tests were carried out between 170 and 290°C and confirmed complete reactions in less than 10 min with an overall NH₃ yield increasing with temperature (~14 mmol/g when the temperature was maintained above 200°C during hydrolysis), as shown in Figure S15. The measured NH₃ production thus corresponds to about 100% of the theoretical maximum production when the temperature is high enough.

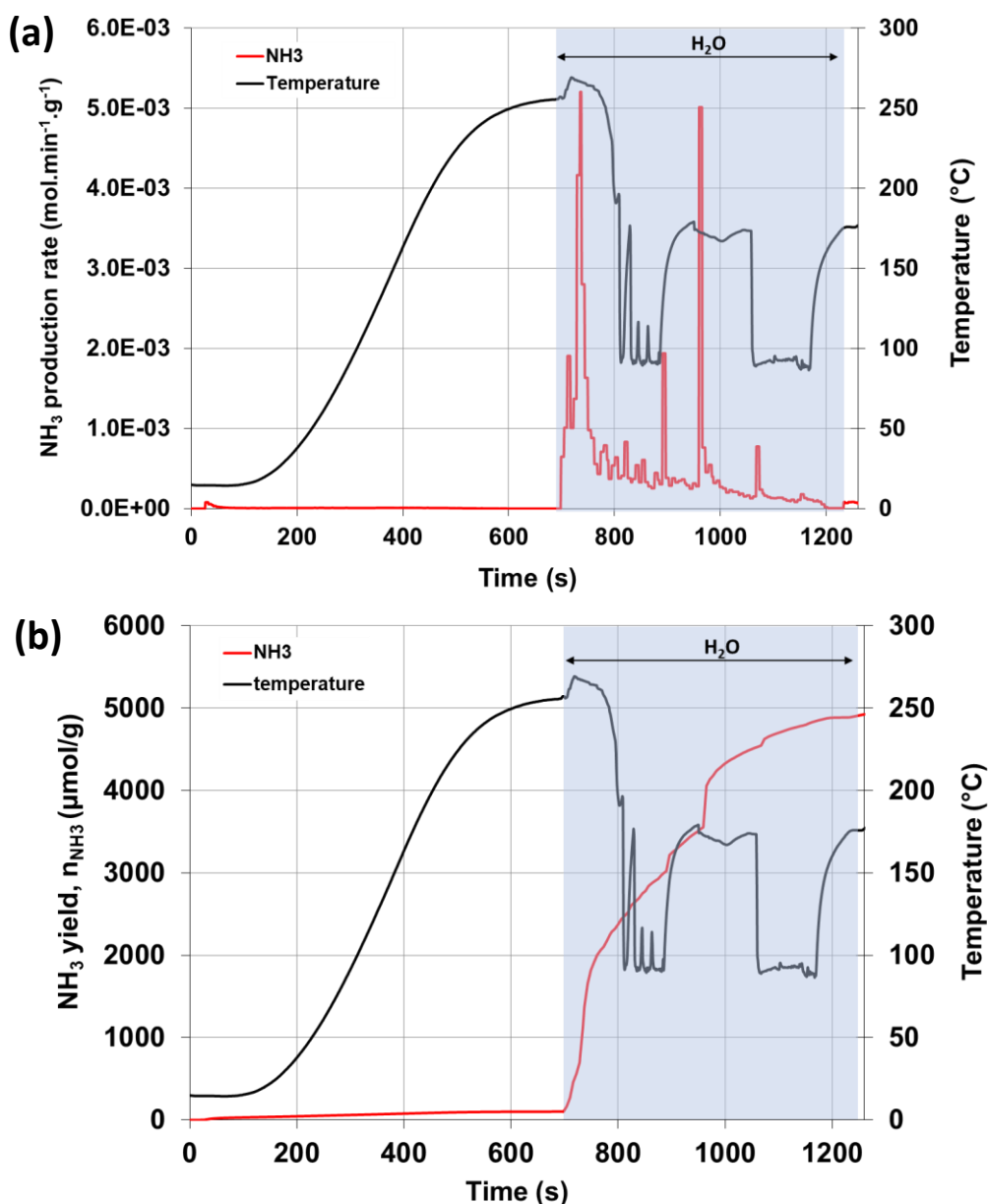


Figure 6. NH₃ production during Ca₃N₂ hydrolysis at 260°C: (a) evolution of NH₃ production rate as a function of time, (b) cumulative NH₃ production as a function of time.

The material was characterized by XRD before and after hydrolysis at different temperatures to identify the existing phases and compare with the fresh material (Figure 7). Whatever the hydrolysis temperature (160°C, 200°C or 250°C), the nitride phase disappeared and Ca(OH)₂ was the main phase identified, which denotes a total oxidation of the nitride (and a hydration of CaO). A complete conversion of the nitride with water was thus confirmed by XRD. A tetragonal ZrO₂ phase was also detected, due to zirconia felt as a powder support in the reactor. Also note the absence of CaO, as calcium hydroxide is stable and does not decompose at these temperatures.

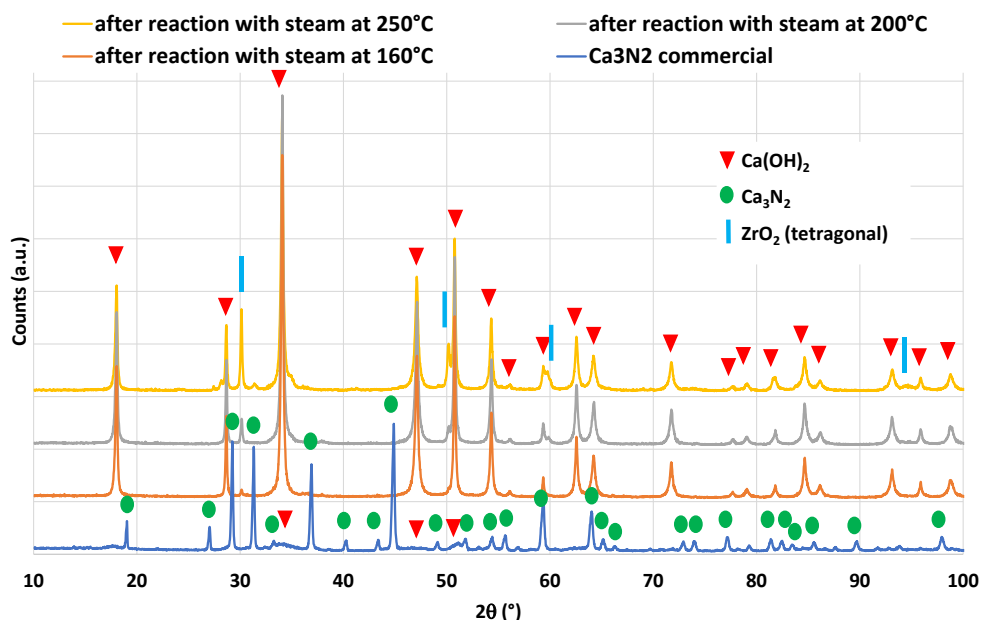


Figure 7. XRD patterns of calcium nitride powders before and after hydrolysis at different temperatures.

EDX analysis of the powder hydrolyzed at 270°C was carried out. Table S4 reports the atomic composition of the powder, which shows the absence of nitrogen trace in the sample thus confirming the complete nitride conversion. With a composition of 33%_{at} Ca and 65.7%_{at} O, the Ca/O ratio is 0.5, thus corresponding to the atomic ratio in Ca(OH)₂. Traces of zirconium are also detected and correspond to the powder felt support used during the tests. Figure S16 shows the SEM and EDX elemental mapping of the sample composed of Ca and O evenly distributed on the surface.

3.5 Magnesium nitride (Mg₃N₂)

The hydrolysis reaction of commercial magnesium nitride (101 mg) was studied, with the following overall equations:



The calculated maximum NH₃ production is 19.8.10⁻³ mol/g. Figure 8 shows the NH₃ production profile during the hydrolysis of Mg₃N₂ at 190°C. During steam injection, the temperature dropped rapidly due to water vaporization. A substantial production of NH₃ was measured with a maximum peak rate of 1.8.10⁻² mol/min/g and an overall reaction duration of less than 10 min, as confirmed by the NH₃ production returning to zero before the end of steam injection. The cumulative production of NH₃ during Mg₃N₂ hydrolysis at 190°C was 18.6.10⁻³ mol/g (Figure 8b), which corresponds to 94% of the maximum theoretical NH₃ yield.

Other tests were also carried out at slightly different temperatures (from 120 to 275°C) and confirmed the repeatability of the results with complete conversion achieved after about 5 to 10 min of hydrolysis reaction.

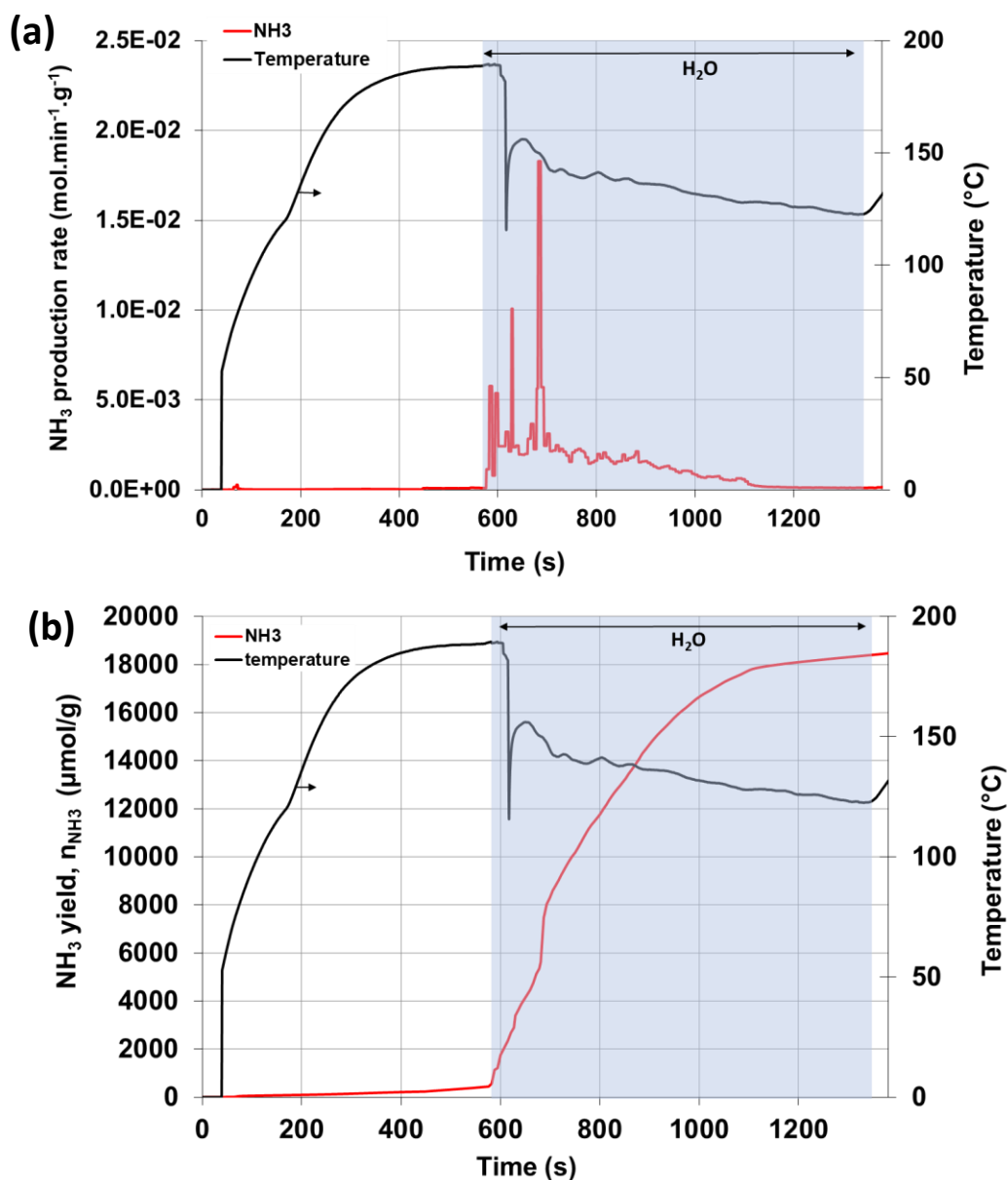


Figure 8. NH_3 production during Mg_3N_2 hydrolysis at 190°C : (a) evolution of NH_3 production rate as a function of time, (b) cumulative NH_3 production as a function of time.

The magnesium nitride powder was characterized by XRD before and after hydrolysis at different temperatures in order to identify the main phases after reaction and to compare them with the pristine material (Figure 9). The nitride phase completely disappeared after reaction whatever the temperature (200°C or 270°C) and both MgO and $\text{Mg}(\text{OH})_2$ were formed, which demonstrates the complete nitride conversion. The peaks related to MgO were higher than those related to $\text{Mg}(\text{OH})_2$ at the highest temperature, which highlights the decomposition of $\text{Mg}(\text{OH})_2$ to MgO with increasing temperature. Some ZrO_2 (tetragonal) from the felt support was also detected, as already mentioned previously for the other materials.

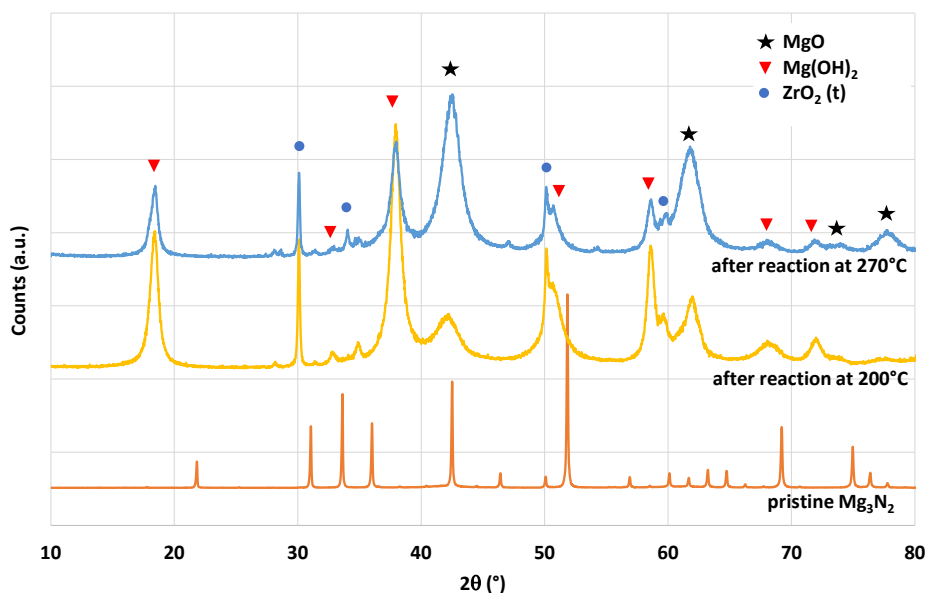


Figure 9. XRD patterns of magnesium nitride powders before and after hydrolysis at different temperatures.

EDX analysis of the powder hydrolyzed at 270°C was performed and the atomic composition is reported in Table S5. No trace of nitrogen was detected, which confirms the complete nitride conversion. With a composition of 35.3%_{at} Mg and 61.6%_{at} O, the Mg/O ratio is 0.57, corresponding to an intermediate ratio between MgO and Mg(OH)₂ in agreement with the results of XRD analysis. Traces of zirconium are also detected corresponding to the felt support.

Figure S17 shows SEM and EDX elemental mapping related to the atomic composition of the sample. The powder is composed of Mg and O evenly distributed over the surface.

3.6 Titanium nitride (TiN)

Titanium nitride was considered for solar production of NH₃, with the following hydrolysis reaction equation:



Titanium can also form oxy-nitride species of varying composition and stoichiometry, which can impact the overall equation. Based on Eq. (27), the theoretical maximum production of NH₃ is 16.1.10⁻³ mol/g. According to thermodynamics (Fig. S18), the formation of NH₃ is only predicted below 300°C because it decomposes at higher temperatures, and secondary oxide and oxy-nitride minor phases are predicted at higher temperatures (above ~800°C).

Figure 10a shows the evolution of the NH₃ production rate during TiN hydrolysis at 900°C, 970°C, and 1000°C. Although the reaction was not thermodynamically favored at high temperatures, the peak production rate increased with increasing temperature due to a kinetically-controlled reaction. The NH₃ production rate rose from 2.4.10⁻⁴ mol/min/g at 900°C, to 3.4.10⁻³ mol/min/g at 1000°C. The reaction duration was short whatever the temperature since NH₃ production was completed in less than ~3-4 min, indicating fast kinetics. Other hydrolysis reactions carried out at 250°C and 500°C did not produce NH₃, which means that the temperature must be high enough to obtain noticeable kinetics. Figure 10b shows the cumulative production of NH₃ during TiN hydrolysis at different temperatures. The NH₃ production increased significantly with temperature as it was 2.16 mmol/g at 900°C, 3.06 mmol/g at 970°C, and 4.05 mmol/g at 1000°C.

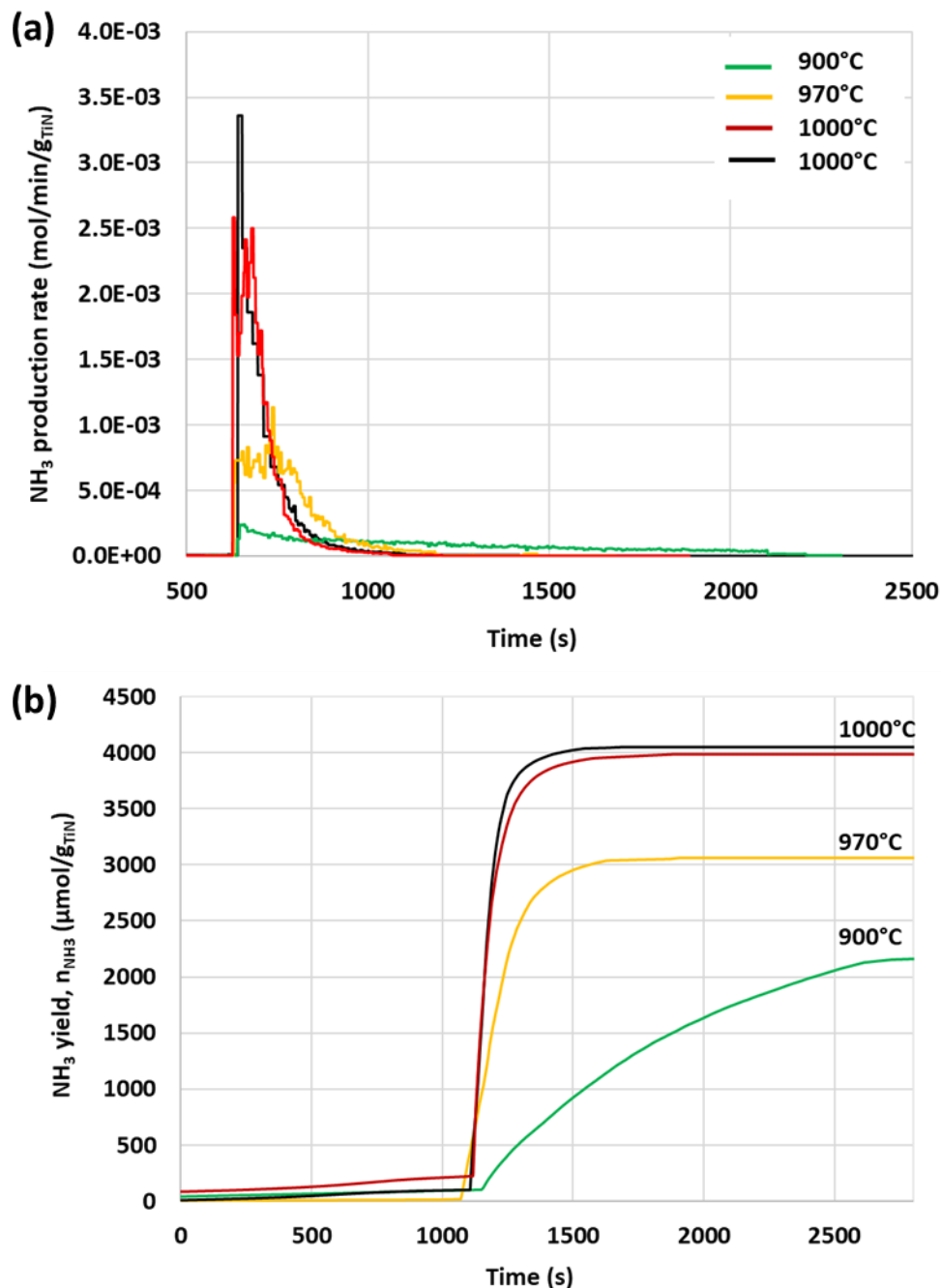


Figure 10. NH_3 production during TiN hydrolysis at 900°C, 970°C and 1000°C: (a) evolution of NH_3 production rate as a function of time, (b) cumulative NH_3 production as a function of time.

XRD analysis of titanium nitride powders before and after hydrolysis at different temperatures was carried out (Figure 11). TiO_2 (rutile) was observed as the main phase after hydrolysis at each temperature considered. The initial TiN phase was still detected at 900°C but remained in very low amount. The intensity of TiN peaks relative to TiO_2 decreased when temperature increased, confirming an improvement in reaction extent. $\text{ZrO}_2(\text{t})$ from the felt support was also detected, consistently with previous results.

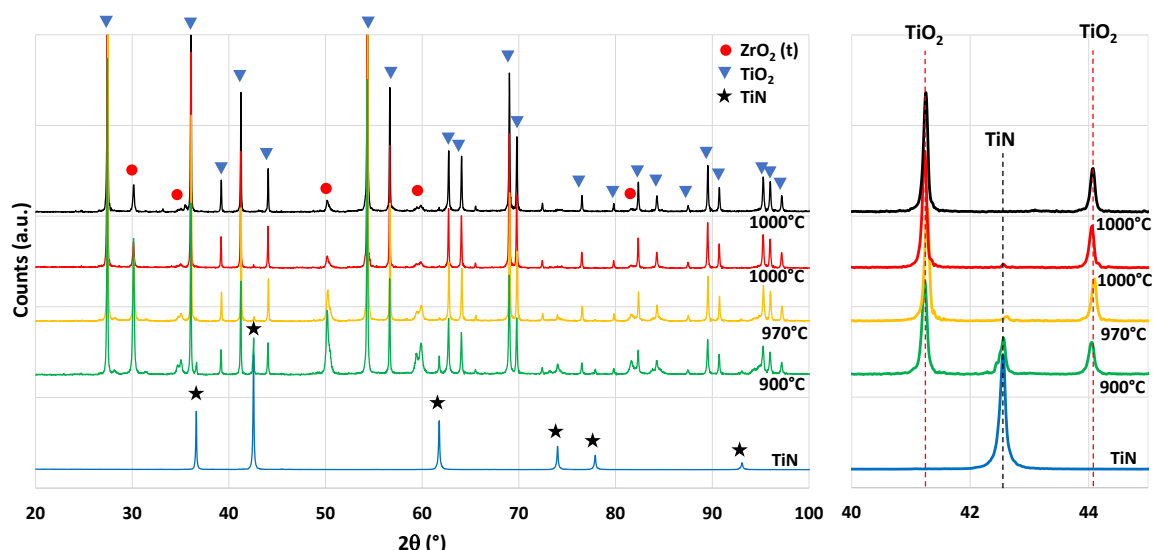


Figure 11. XRD patterns of TiN powders before and after hydrolysis at different temperatures.

EDX analysis of TiN powders hydrolyzed at 900°C, 970°C, and 1000°C was performed and Table S6 reports the atomic compositions. The Ti/O ratio is 0.52 at 1000°C, corresponding approximately to TiO₂ composition. No trace of nitrogen was detected at any hydrolysis temperature, which means it is below the detection limit. The traces of zirconium correspond to the felt support.

Figures S19-S21 show the SEM and EDX elemental mapping of powders hydrolyzed at 900, 930 and 1000°C, confirming the homogeneous distribution of the Ti and O elements.

3.7 Zirconium nitride (ZrN)

The final material tested in this study of nitride hydrolysis for NH₃ production was zirconium nitride (ZrN).



As for Ti, Zr can form oxy-nitrides which can modify the overall equation of the reaction. Based on Eq. (28), the theoretical maximum production of NH₃ is $11.0 \cdot 10^{-3} \text{ mol/g}$.

The NH₃ production profiles during ZrN hydrolysis were studied at 550°C, 620°C, 750°C, 820°C, 920°C, and 1000°C (Figures 12 and S22). An increase in the peak production rate was measured until it reached an optimum at 750°C and decreased at higher temperatures (Table 1). The maximum NH₃ production rate at 750°C reached 34.2 mmol/min/g (767 mL/min/g), which was the highest reaction rate obtained among the nitrides tested. The period of NH₃ production was short, as the reaction was completed in less than about 2-3 min, except at the lowest temperature of 550°C where the kinetics were much slower. Figure 12b reports the cumulative production of NH₃ during ZrN hydrolysis at different temperatures, with an optimum at 750°C corresponding to a maximum NH₃ production yield of 12.3 mmol/g (Fig. S23).

Table 1. Peak production rates and yields of NH₃ during ZrN hydrolysis at different temperatures.

	Peak production rate (mmol/min/g)	Peak production rate (mL/min/g)	Yield of NH ₃ (mmol/g)
550°C	0.50	11.3	7.9
620°C	17.6	393.4	11.4
750°C	34.2	767.0	12.3
820°C	21.8	488.9	11.2
920°C	25.1	562.2	8.3
1000°C	15.7	352.9	2.1
1010°C	1.16	26.0	0.75

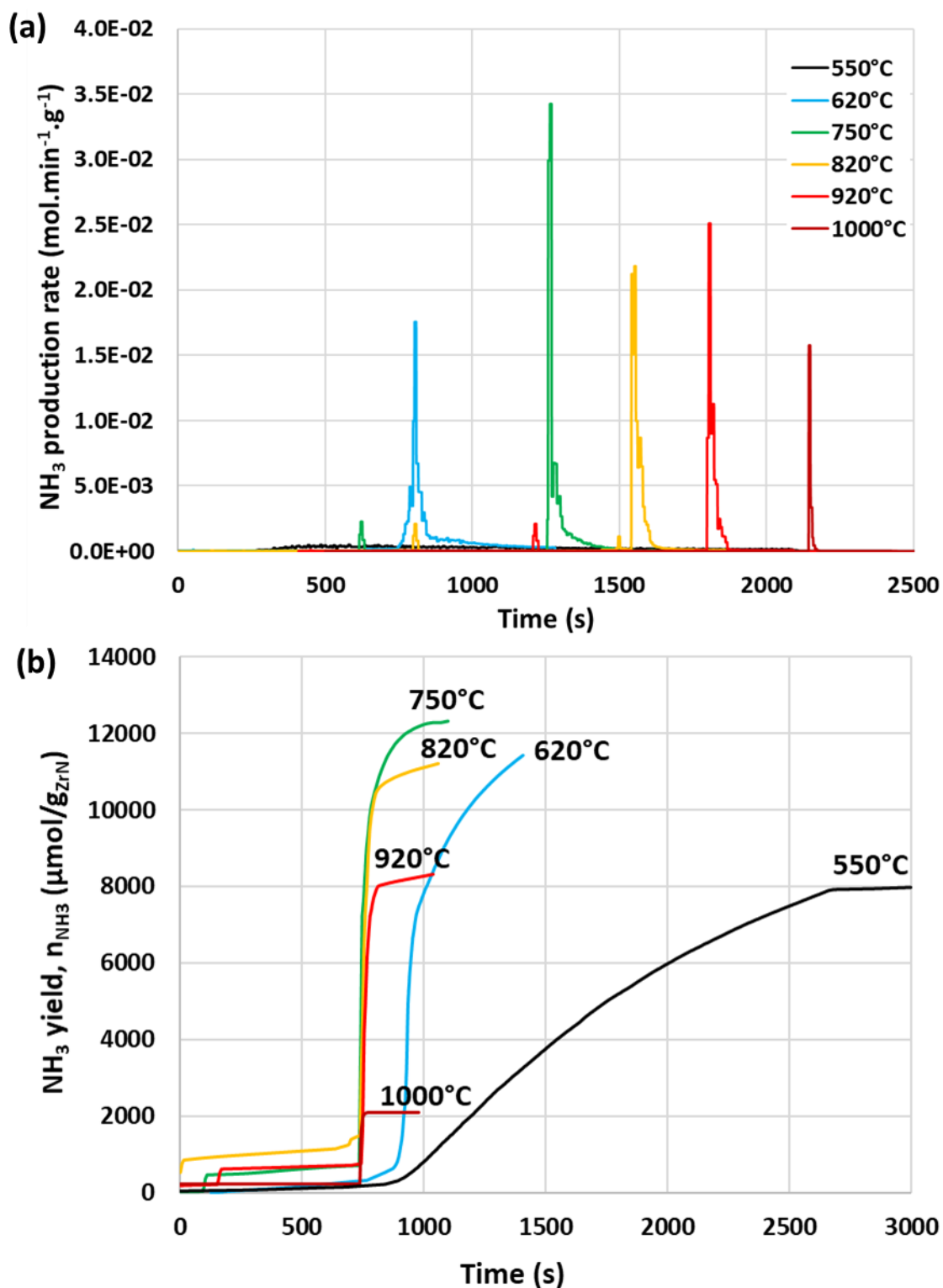


Figure 12. NH_3 production during ZrN hydrolysis at different temperatures: (a) comparison of NH_3 production rate, (b) cumulative NH_3 production as a function of time.

XRD analysis of zirconium nitride powders before and after hydrolysis at different temperatures (Figure 13) shows that ZrO_2 (monoclinic and tetragonal) is the main phase after the reaction at any temperature. The intensity ratio of peaks related to monoclinic ZrO_2 increases with temperature. The initial ZrN phase is still observed especially at 550°C and 620°C, and it disappears at higher temperatures, which confirms the enhanced hydrolysis extent when increasing the temperature.

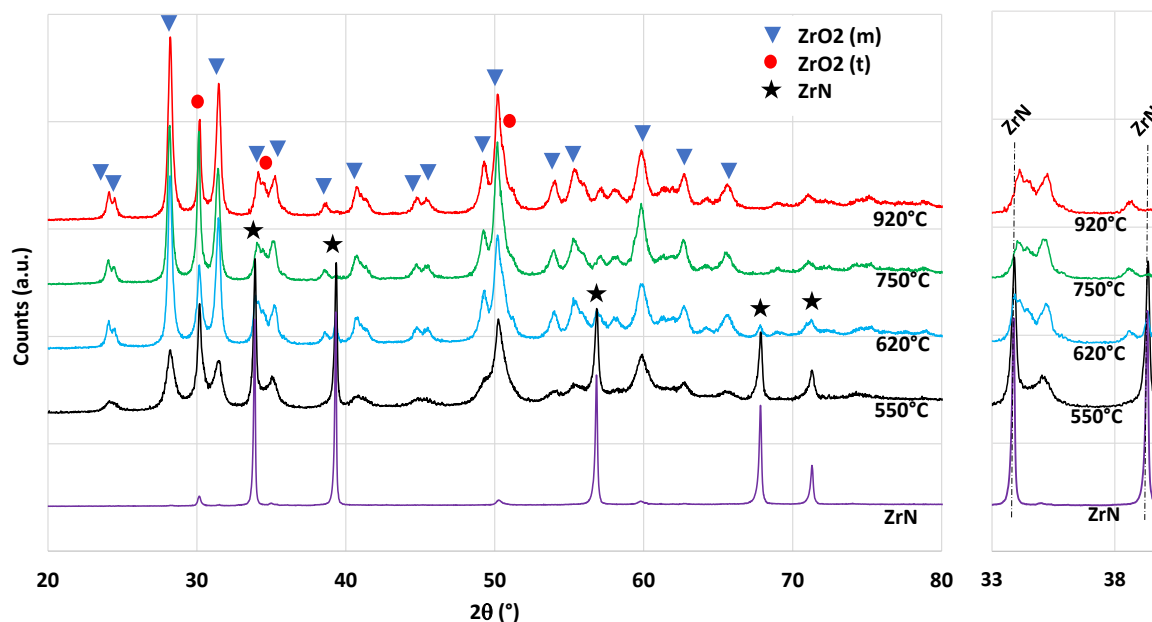


Figure 13. XRD patterns of ZrN powders before and after hydrolysis at different temperatures.

EDX analysis of powders hydrolyzed at 620°C, 750°C, 820°C, and 920°C was performed and Table S7 reports the atomic composition, confirming the overall ZrO₂ composition after hydrolysis (Zr/O ratio of ~0.5). Some nitrogen was always detected, except for the powder hydrolyzed at 750°C, in agreement with the maximum conversion observed at this temperature.

Figures S24-S27 show the SEM and EDX elemental mapping of powders hydrolyzed at 620, 750, 820, and 920°C. A homogeneous distribution of Zr, O and N is evidenced.

This study successfully demonstrated the production of ammonia from the hydrolysis of ZrN with fast rates and optimum conversion at 750°C. The next step will focus on the solar regeneration of nitrides from ZrO₂ oxide.

4. Conclusion

The production of ammonia via two-step cycles relying on N₂ and H₂O as the only feedstocks is an attractive approach, as it uses solar heat as the process energy input and additionally bypasses the use of H₂. Active materials involved in such thermochemical cycles (metal oxide/nitride redox pairs) must be identified and optimized to demonstrate the feasibility of the solar ammonia production process. A series of ten metal nitrides was experimentally tested for ammonia production from nitrides hydrolysis. Iron (FeN), chromium (CrN), boron (BN), and silicon (Si₃N₄) nitrides gave no significant NH₃ production, and therefore cannot be considered as suitable candidate materials for thermochemical ammonia production cycles. Among the considered nitrides, the most attractive materials turned out to be AlN, Li₃N, Ca₃N₂, Mg₃N₂, TiN, and ZrN because they exhibit a noteworthy reactivity during hydrolysis and a significant production of NH₃. The influence of temperature was studied for each material and proved to have a strong impact on the reaction conversion and the NH₃ yield. AlN hydrolysis occurred significantly above 1000°C with maximum rates at 1200°C (0.16 mmol/min/g), but the NH₃ yield remained moderate (1.1 mmol/g) presumably due to decomposition at high temperatures. TiN and ZrN also required high temperatures for NH₃ production. A maximum NH₃ production rate of 3.4 mmol/min/g was measured at 1000°C for TiN (NH₃ yield of 4.1 mmol/g), while an optimum temperature of 750°C was revealed for ZrN yielding the highest NH₃ production rate of 34.2 mmol/min/g (NH₃ yield of 12.3 mmol/g). The hydrolysis reactions of Li₃N, Ca₃N₂, and Mg₃N₂ were the most exothermic and thus required low temperatures (around 200°C) to achieve complete conversion, with total NH₃ yields of 5.9, 4.9, and 18.6 mmol/g, respectively. The hydrolysis rate of Ca₃N₂ and Mg₃N₂ was slightly lower than that of Li₃N, TiN, and ZrN.

This study thus demonstrated the feasibility of sustainable ammonia synthesis from a novel clean process ultimately based on concentrated solar energy as the process heat source. Noteworthy ammonia production performance was achieved with the identified metal nitrides. Thermochemical ammonia production based on nitrides cycles is a suitable means for industrial process decarbonation. Future work will focus on the regeneration step of the metal nitrides using concentrated solar energy at high temperatures. The most reactive nitrides were found to be Li₃N,

Ca₃N₂, Mg₃N₂, TiN and ZrN. The solar-driven nitridation reaction of the corresponding oxides (Li₂O, CaO, MgO, TiO₂, and ZrO₂) must therefore be characterized as a function of temperature and reducing agent to demonstrate the complete cycles of nitride chemical looping for ammonia synthesis.

Declaration of Competing Interest

The authors declare that they have no known competing financial interests or personal relationships that could have appeared to influence the work reported in this paper.

Acknowledgments

This work was partially funded by the CNRS Energy Unit (Cellule Energie) through the PEPS AMMOSOL project. The authors acknowledge the support from the PCM characterization platform (E. Bêche) at PROMES-CNRS during the XRD analysis.

Appendix A. Supplementary material

The following is the Supplementary material related to this article.

Supplementary material contains a summary of the experimental conditions and the corresponding total amounts of NH₃ produced during the different hydrolysis tests, additional NH₃ production data for metal nitrides hydrolysis, materials characterization including XRD analysis data and SEM/EDX imaging/elemental mapping.

Data availability

Data will be made available on request.

References

- Abanades, S., 2023. A Review of Oxygen Carrier Materials and Related Thermochemical Redox Processes for Concentrating Solar Thermal Applications. *Materials* 16, 3582. <https://doi.org/10.3390/ma16093582>
- Abanades, S., 2022. Redox Cycles, Active Materials, and Reactors Applied to Water and Carbon Dioxide Splitting for Solar Thermochemical Fuel Production: A Review. *Energies* 15, 7061. <https://doi.org/10.3390/en15197061>
- Aziz, M., Wijayanta, A.T., Nandiyanto, A.B.D., 2020. Ammonia as Effective Hydrogen Storage: A Review on Production, Storage and Utilization. *Energies* 13, 3062. <https://doi.org/10.3390/en13123062>
- Bartel, C.J., Rumpitz, J.R., Weimer, A.W., Holder, A.M., Musgrave, C.B., 2019. High-Throughput Equilibrium Analysis of Active Materials for Solar Thermochemical Ammonia Synthesis. *ACS Appl. Mater. Interfaces* 11, 24850–24858. <https://doi.org/10.1021/acsami.9b01242>
- Bhaskar, A., Assadi, M., Nikpey Somehsaraei, H., 2020. Decarbonization of the Iron and Steel Industry with Direct Reduction of Iron Ore with Green Hydrogen. *Energies* 13, 758. <https://doi.org/10.3390/en13030758>
- Ceballos, B.M., Pilania, G., Ramaiyan, K.P., Banerjee, A., Kreller, C., Mukundan, R., 2021. Roads less traveled: Nitrogen reduction reaction catalyst design strategies for improved selectivity. *Current Opinion in Electrochemistry* 28, 100723. <https://doi.org/10.1016/j.coelec.2021.100723>
- Chambon, M., Abanades, S., Flamant, G., 2010a. Solar thermal reduction of ZnO and SnO₂: Characterization of the recombination reaction with O₂. *Chemical Engineering Science* 65, 3671–3680. <https://doi.org/10.1016/j.ces.2010.03.005>
- Chambon, M., Abanades, S., Flamant, G., 2010b. Design of a Lab-Scale Rotary Cavity-Type Solar Reactor for Continuous Thermal Dissociation of Volatile Oxides Under Reduced Pressure. *Journal of Solar Energy Engineering* 132, 021006. <https://doi.org/10.1115/1.4001147>
- Chuayboon, S., Abanades, S., 2019. Clean magnesium production using concentrated solar heat in a high-temperature cavity-type thermochemical reactor. *Journal of Cleaner Production* 232, 784–795. <https://doi.org/10.1016/j.jclepro.2019.05.371>
- Daisley, A., Hargreaves, J.S.J., 2023. Metal nitrides, the Mars-van Krevelen mechanism and heterogeneously catalysed ammonia synthesis. *Catalysis Today* 423, 113874. <https://doi.org/10.1016/j.cattod.2022.08.016>

- Damanabi, A.T., Servatan, M., Mazinani, S., Olabi, A.G., Zhang, Z., 2019. Potential of tri-reforming process and membrane technology for improving ammonia production and CO₂ reduction. *Science of The Total Environment* 664, 567–575. <https://doi.org/10.1016/j.scitotenv.2019.01.391>
- Gálvez, M.E., Frei, A., Halmann, M., Steinfeld, A., 2007a. Ammonia Production via a Two-Step Al₂O₃/AlN Thermochemical Cycle. 2. Kinetic Analysis. *Ind. Eng. Chem. Res.* 46, 2047–2053. <https://doi.org/10.1021/ie061551m>
- Gálvez, M.E., Halmann, M., Steinfeld, A., 2007b. Ammonia Production via a Two-Step Al₂O₃/AlN Thermochemical Cycle. 1. Thermodynamic, Environmental, and Economic Analyses. *Ind. Eng. Chem. Res.* 46, 2042–2046. <https://doi.org/10.1021/ie061550u>
- Gálvez, M.E., Hischer, I., Frei, A., Steinfeld, A., 2008. Ammonia Production via a Two-Step Al₂O₃/AlN Thermochemical Cycle. 3. Influence of the Carbon Reducing Agent and Cyclability. *Ind. Eng. Chem. Res.* 47, 2231–2237. <https://doi.org/10.1021/ie071244w>
- Goto, Y., Daisley, A., Hargreaves, J.S.J., 2021. Towards anti-perovskite nitrides as potential nitrogen storage materials for chemical looping ammonia production: Reduction of Co₃ZnN, Ni₃ZnN, Co₃InN and Ni₃InN under hydrogen. *Catalysis Today* 364, 196–201. <https://doi.org/10.1016/j.cattod.2020.03.022>
- Haeussler, A., Abanades, S., Jouannaux, J., Drobek, M., Ayral, A., Julbe, A., 2019. Recent progress on ceria doping and shaping strategies for solar thermochemical water and CO₂ splitting cycles. *AIMS Materials Science* 6, 657–684. <https://doi.org/10.3934/mat.2019.5.657>
- Hunter, S.M., McKay, D., Smith, R.I., Hargreaves, J.S.J., Gregory, D.H., 2010. Topotactic Nitrogen Transfer: Structural Transformation in Cobalt Molybdenum Nitrides. *Chem. Mater.* 22, 2898–2907. <https://doi.org/10.1021/cm100208a>
- Jain, A., Miyaoka, H., Kumar, S., Ichikawa, T., Kojima, Y., 2017. A new synthesis route of ammonia production through hydrolysis of metal – Nitrides. *International Journal of Hydrogen Energy* 42, 24897–24903. <https://doi.org/10.1016/j.ijhydene.2017.08.027>
- Kishira, S., Qing, G., Suzu, S., Kikuchi, R., Takagaki, A., Oyama, S.T., 2017. Ammonia synthesis at intermediate temperatures in solid-state electrochemical cells using cesium hydrogen phosphate based electrolytes and noble metal catalysts. *International Journal of Hydrogen Energy* 42, 26843–26854. <https://doi.org/10.1016/j.ijhydene.2017.09.052>
- Klaas, L., Guban, D., Roeb, M., Sattler, C., 2021. Recent progress towards solar energy integration into low-pressure green ammonia production technologies. *International Journal of Hydrogen Energy* 46, 25121–25136. <https://doi.org/10.1016/j.ijhydene.2021.05.063>
- Kyriakou, V., Garagounis, I., Vasileiou, E., Vourros, A., Stoukides, M., 2017. Progress in the Electrochemical Synthesis of Ammonia. *Catalysis Today* 286, 2–13. <https://doi.org/10.1016/j.cattod.2016.06.014>
- Laassiri, S., Zeinalipour-Yazdi, C.D., Catlow, C.R.A., Hargreaves, J.S.J., 2018. The potential of manganese nitride based materials as nitrogen transfer reagents for nitrogen chemical looping. *Applied Catalysis B: Environmental* 223, 60–66. <https://doi.org/10.1016/j.apcatb.2017.04.073>
- Lai, Q., Cai, T., Tsang, S.C.E., Chen, X., Ye, R., Xu, Z., Argyle, M.D., Ding, D., Chen, Y., Wang, J., Russell, A.G., Wu, Y., Liu, J., Fan, M., 2022. Chemical looping based ammonia production—A promising pathway for production of the noncarbon fuel. *Science Bulletin* 67, 2124–2138. <https://doi.org/10.1016/j.scib.2022.09.013>
- Le Gal, A., Abanades, S., 2011. Catalytic investigation of ceria-zirconia solid solutions for solar hydrogen production. *International Journal of Hydrogen Energy* 36, 4739–4748. <https://doi.org/10.1016/j.ijhydene.2011.01.078>
- Liu, X., Elgowainy, A., Wang, M., 2020. Life cycle energy use and greenhouse gas emissions of ammonia production from renewable resources and industrial by-products. *Green Chem.* 22, 5751–5761. <https://doi.org/10.1039/D0GC02301A>
- Marnellos, G., Stoukides, M., 1998. Ammonia Synthesis at Atmospheric Pressure. *Science* 282, 98–100. <https://doi.org/10.1126/science.282.5386.98>
- Marnellos, G., Zisekas, S., Stoukides, M., 2000. Synthesis of Ammonia at Atmospheric Pressure with the Use of Solid State Proton Conductors. *Journal of Catalysis* 193, 80–87. <https://doi.org/10.1006/jcat.2000.2877>
- Michalsky, R., Avram, A.M., Peterson, B.A., Pfromm, P.H., Peterson, A.A., 2015a. Chemical looping of metal nitride catalysts: low-pressure ammonia synthesis for energy storage. *Chem. Sci.* 6, 3965–3974. <https://doi.org/10.1039/C5SC00789E>

- Michalsky, R., Parman, B.J., Amanor-Boadu, V., Pfromm, P.H., 2012. Solar thermochemical production of ammonia from water, air and sunlight: Thermodynamic and economic analyses. *Energy* 42, 251–260. <https://doi.org/10.1016/j.energy.2012.03.062>
- Michalsky, R., Pfromm, P.H., 2011. Chromium as reactant for solar thermochemical synthesis of ammonia from steam, nitrogen, and biomass at atmospheric pressure. *Solar Energy* 85, 2642–2654. <https://doi.org/10.1016/j.solener.2011.08.005>
- Michalsky, R., Pfromm, P.H., Steinfeld, A., 2015b. Rational design of metal nitride redox materials for solar-driven ammonia synthesis. *Interface Focus* 5, 20140084. <https://doi.org/10.1098/rsfs.2014.0084>
- Michalsky, R., Steinfeld, A., 2017. Computational screening of perovskite redox materials for solar thermochemical ammonia synthesis from N₂ and H₂O. *Catalysis Today* 286, 124–130. <https://doi.org/10.1016/j.cattod.2016.09.023>
- Mordor Intelligence LLP, 2021. Ammonia Market - Growth, Trends, COVID-19 Impact, and Forecasts (2021 - 2026) (No. 6036753).
- Murakami, T., Nishikiori, T., Nohira, T., Ito, Y., 2003. Electrolytic Synthesis of Ammonia in Molten Salts under Atmospheric Pressure. *J. Am. Chem. Soc.* 125, 334–335. <https://doi.org/10.1021/ja028891t>
- Murakami, T., Nohira, T., Ogata, Y.H., Ito, Y., 2005a. Electrolytic Ammonia Synthesis in Molten Salts under Atmospheric Pressure Using Methane as a Hydrogen Source. *Electrochem. Solid-State Lett.* 8, D12. <https://doi.org/10.1149/1.1870633>
- Murakami, T., Nohira, T., Ogata, Y.H., Ito, Y., 2005b. Electrochemical Synthesis of Ammonia and Coproduction of Metal Sulfides from Hydrogen Sulfide and Nitrogen under Atmospheric Pressure. *J. Electrochem. Soc.* 152, D109. <https://doi.org/10.1149/1.1904984>
- Murray, J., Steinfeld, A., Fletcher, E., 1995. Metals, nitrides, and carbides via solar carbothermal reduction of metal oxides. *Energy* 20, 695–704. [https://doi.org/10.1016/0360-5442\(95\)00032-C](https://doi.org/10.1016/0360-5442(95)00032-C)
- Patisson, F., Mirgaux, O., 2020. Hydrogen Ironmaking: How It Works. *Metals* 10, 922. <https://doi.org/10.3390/met10070922>
- Qing, G., Kikuchi, R., Kishira, S., Takagaki, A., Sugawara, T., Oyama, S.T., 2016. Ammonia Synthesis by N₂ and Steam Electrolysis in Solid-State Cells at 220°C and Atmospheric Pressure. *J. Electrochem. Soc.* 163, E282–E287. <https://doi.org/10.1149/2.0161610jes>
- Rafiqul, I., Weber, C., Lehmann, B., Voss, A., 2005. Energy efficiency improvements in ammonia production—perspectives and uncertainties. *Energy* 30, 2487–2504. <https://doi.org/10.1016/j.energy.2004.12.004>
- Wang, L., Xia, M., Wang, H., Huang, K., Qian, C., Maravelias, C.T., Ozin, G.A., 2018. Greening Ammonia toward the Solar Ammonia Refinery. *Joule* 2, 1055–1074. <https://doi.org/10.1016/j.joule.2018.04.017>
- Xiao, L., Wu, S.-Y., Li, Y.-R., 2012. Advances in solar hydrogen production via two-step water-splitting thermochemical cycles based on metal redox reactions. *Renewable Energy* 41, 1–12. <https://doi.org/10.1016/j.renene.2011.11.023>
- Yang, S., Zhang, T., Yang, Y., Wang, B., Li, J., Gong, Z., Yao, Z., Du, W., Liu, S., Yu, Z., 2022. Molybdenum-based nitrogen carrier for ammonia production via a chemical looping route. *Applied Catalysis B: Environmental* 312, 121404. <https://doi.org/10.1016/j.apcatb.2022.121404>